Hydro-mechanical modelling of gas migration in host rocks for nuclear waste repositories

Jianxiong Yang[1], Mamadou Fall[1*]
1. Department of Civil Engineering, University of Ottawa, Ottawa, On, Canada
*Corresponding author: 161 Louis Pasteur, Ottawa, Ontario, Canada K1N6N5, mfall@uottawa.ca

Abstract: Deep geological repositories (DGRs) are currently being proposed in several countries to deal with the nuclear waste. The safe long-term disposal of the waste is guaranteed by a multi-barrier system, which includes a natural barrier (host rocks) and an engineered barrier system. Large quantities of gas can be generated during the lifespan of the DGRs due to several processes, such as the corrosion of metal, water radiolysis or microbial degradation. The generated gas could potentially overpressurize the DGR, deteriorate the hydraulic and mechanical properties of the host rock and impact the long term safety of the DGR. Thus, the understanding and prediction of gas migration within the host rock and associated potential impacts on its integrity is critical for the long term safety of a DGR. Numerous laboratory tests have shown that gas migration in host rock involves complex hydro-mechanical (HM) processes, and the classical concepts of two-phase flow in porous medium is inappropriate to predict this gas migration as well as capture the key HM processes. In the study, a coupled HM model, based on double-porosity approach, is developed and implemented into COMSOL Multiphysics® software to assess and predict gas migration in sedimentary host rocks (claystone). The model takes into account the HM behavior of both the porous medium (representing the matrix) and the fractured medium (representing the fractures). The prediction capability of the model is tested against laboratory gas migration tests conducted on potential host sedimentary rocks (claystone). The simulated results are in good agreement with the experimental data, which shows the robustness of the developed model. The validation results have also shown that the developed model can well capture the main experimental observations, such as the development of gas preferential pathways and gas induced fracturing.

Keywords: deep geological repository for nuclear waste; double porosity; double effective stress; hydro-mechanical processes; gas induced fracturing

1. Introduction

As a promising option to dispose the nuclear waste, deep geological repositories (DGRs) have been proposed or currently being constructed in several countries, including Canada, France, Germany, India and Switzerland . An important basis of the DGRs is the proposition of multi-barrier concept, which consists of engineered barrier system and natural barrier system (host rock) [1]. Each barrier represents an additional impediment to the waste migration, in which host rock is the final impediment. The highly consolidated argillaceous formation, the Callovo-Oxfordian (COx) clay, is being investigated as a host rock due to its suitable thickness and good radionuclide retardation capability. However, the integrity of the host rock may be affected by the gas generated due to the corrosion of metal, water radiolysis or microbial degradation [2,3]. As micro-fractures or macro-fractures gradually develop in the rock mass, the gas could migrate through the rock, and the gas preferential pathways may form, accordingly enable the easy transport of the radioactive contaminants and significantly impact the biosphere and groundwater. Therefore, investigating the gas migration process in host rocks is important for assessing the long-term safety of DGRs.

As gas migrates within the initial saturated rock, two phase (gas, water) flow process and gas induced micro-fracture could occur. Accordingly, the numerical simulation of gas migration needs to consider both the coupled HM process and the micro-fracturing process. Thus, a new coupled HM model based on double porosity approach and concept of double effective stress is proposed in the study. This model considers the deformation of both the porous medium (representing the matrix) and the fractured medium (representing the fractures) as well as fluid flow in pores and fractures. The predictive ability of the model is then evaluated by simulating a gas injection test in saturated claystone, and then comparing the simulation results against the laboratory results. Good agreement is achieved between the simulated and laboratory results, which show the robustness of the model.

2. Double Porosity Approach

Natural rock mass usually contains joints and fractures at different scales, which largely affects the pore size distribution (PSD) of the porous medium. To better simulate the process of gas migration in host rocks, the rock is viewed as a double porosity system, which enable to take into account the HM behavior of both matrix and fracture.

Based on the mixture theory for double porosity media, Biot's theory of poromechanics has been extended to examine fracturing in rocks [4–8]. At the macroscopic level, a fractured porous medium (FPM) is considered to consist of two separate and overlapping porous media: one represents the porous continuum (PC), while the other one represents the fractured continuum (FC), as shown in Figure 1. Each porous medium is assumed to have the self-governed properties, such as the elastic modulus and Biot's effective stress coefficient. A representative elementary volume (REV) is used to describe the FPM, see Figure 1. The total volume, V_t, overall bulk modulus, K, and shear modulus, G of the FPM are given as follows [7–9],

$$V_t = V_{s(p)} + V_p = V_{s(f)} + V_f \tag{1}$$

$$\frac{1}{K} = \frac{1}{K_p} + \frac{1}{K_f} \tag{2}$$

$$\frac{1}{G} = \frac{1}{G_p} + \frac{1}{G_f} \tag{3}$$

where K_p and K_f are the bulk modulus of the PC and the FC respectively. G_p and G_f are the shear modulus of the PC and the FC, respectively.

Two different porosity values are assigned to the PC and FC:

$$\phi_p = \frac{V_p}{V_t},\ \phi_f = \frac{V_f}{V_t} \tag{4}$$

where ϕ_p and ϕ_f are the porosity of the PC and FC, respectively.

3. Governing Equations

In the coupled double porosity HM model, the primary variables are gas pressure in the FC p_{fg}, water pressure in the FC p_{fw}, water pressure in the PC p_{pw}, solid displacement $\mathbf{u}$, ϕ_p and ϕ_f. The governing equations are developed on the background that the constitutive relation of each continuum, i.e., the PC and FC, is governed by themselves independently [8].

3.1 Balance equations

The mass balance equations for gas and water in the FC are written in the following forms, respectively.

$$\rho_{fg}\left(\frac{\phi_f(1-S_e)M}{\rho_{fg}RT} + \phi_f C_s\right)\frac{\partial p_{fg}}{\partial t} + \nabla\cdot(\rho_{fg}\mathbf{v}_{fg}^D) = \rho_{fg}\phi_f C_s\frac{\partial p_{fw}}{\partial t} - \rho_{fg}(1-S_e)(1-\frac{K_f}{K})\frac{\partial \varepsilon_{fv}}{\partial t} \tag{5}$$

$$\rho_{fw}\left(\phi_f S_e \chi_w + \phi_f C_s\right)\frac{\partial p_{fw}}{\partial t} + \nabla\cdot(\rho_{fw}\mathbf{v}_{fw}^D) = \rho_{fw}\phi_f C_s\frac{\partial p_{fg}}{\partial t} - \rho_{fw}S_e(1-\frac{K_f}{K})\frac{\partial \varepsilon_{fv}}{\partial t} + \xi\rho_{fw}(p_{fw}-p_{pw}) \tag{6}$$

where ρ_{fg} and ρ_{fw} are the density of gas and water in the FC, respectively; $\mathbf{v}_{fg}^D$ is Darcy's velocity of gas in the FC, S_e is the effective water saturation degree, ε_{fv} is the volumetric strain of the FC, χ_w is the water compressibility, M is the molar mass of the gas, R is the universal gas constant, T is the absolute temperature (set to 293.15 K), C_s is a specific storage coefficient, ξ is a parameter controls the water flow between the FC and PC.

The pore size is much smaller than the size of fractures, thus Darcy's law for water flow within the pores is neglected here. The PC is assumed

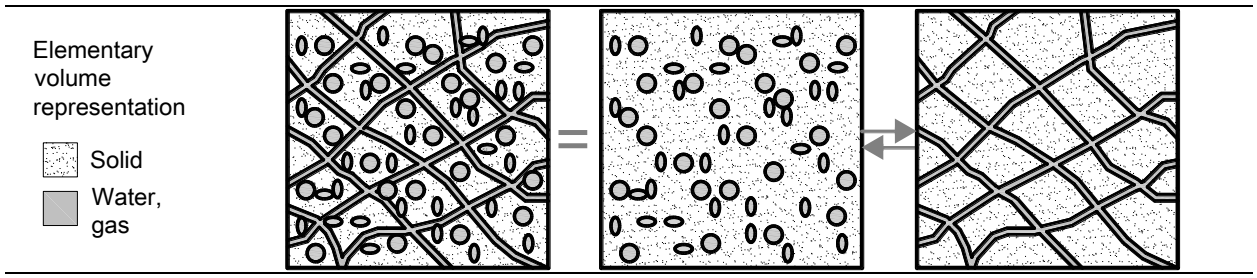

Figure 1. Schematic representation of a mixture with double porosity (modified from [10])

to remain fully saturated throughout the entire process and water can exchange between the PC and FC. The mass balance equation of water in the PC is:

$$\rho_{pw}\phi_p\chi_w\frac{\partial p_{pw}}{\partial t}=-\rho_{pw}(1-\frac{K_p}{K})\frac{\dot{p}_p{}'}{K_p}-\xi\rho_{fw}(p_{fw}-p_{pw}) \quad (7)$$

where ρ_{pw} is the density of water in the PC, $p_p{}'$ is the mean effective pressure of the PC, the overdot represents the time derivative operator.

When the inertial effects and viscous forces are neglected, the momentum balance equation for the FPM is written as

$$\nabla\cdot\dot{\boldsymbol{\sigma}}+\dot{\rho}\mathbf{g}=0 \quad (8)$$

$$\rho=(1-\phi_f-\phi_p)\rho_s+(\phi_f S_e+\phi_p)\rho_w+\phi_f(1-S_e)\rho_g \quad (9)$$

where $\boldsymbol{\sigma}$ is the total stress tensor, $\mathbf{g}$ is the gravity acceleration, ρ is the overall density, ρ_s is the density of the solid grains.

To solve the momentum balance equation, the porosity change is needed here, which is given by

$$\frac{\partial\phi_f}{\partial t}=(1-\frac{K_f}{K}-\phi_f)\frac{\partial\varepsilon_{fv}}{\partial t} \quad (10)$$

$$\frac{\partial\phi_p}{\partial t}=(1-\frac{K_p}{K}-\phi_p)\frac{\dot{p}_p{}'}{K_p} \quad (11)$$

3.2 Constitutive equations

The adopted constitutive relation of the FC is expressed as follows,

$$\mathbf{C}_f:(\boldsymbol{\varepsilon}-\frac{1}{3}\frac{p_p{}'}{K_p}\mathbf{I})=\boldsymbol{\sigma}+(1-\frac{K_f}{K})[S_e p_{fw}+(1-S_e)p_{fg}]\mathbf{I} \quad (12)$$

$$\dot{\boldsymbol{\varepsilon}}=1/2[\nabla\dot{\mathbf{u}}+(\nabla\dot{\mathbf{u}})^T] \quad (13)$$

where $\mathbf{C}_f$ is the elasticity tensor of the FC, $\boldsymbol{\varepsilon}$ is the strain of the FPM, $\mathbf{I}$ is a second order identity tensor.

Fluid flow in the FC is governed by Darcy's law. The change of intrinsic permeability is significant in the gas migration process, which is expressed as follows,

$$\mathbf{k_f}=\mathbf{k_{f0}}\left(\frac{\phi_f}{\phi_{f0}}\right)^3\left(\begin{array}{l} b_1\left(1+\exp\left[b_2(1-\frac{\phi_f-\phi_{f0}}{\phi_{cr}})\right]\right)^{-1}- \\ b_1\left[1+\exp(b_2)\right]^{-1}+1\end{array}\right) \quad (14)$$

where $\mathbf{k_f}$ and $\mathbf{k_{f0}}$ are the intrinsic permeability tensor of the FC and its initial values, respectively; ϕ_{f0} is the initial value of porosity of the FC; b_1, b_2 and ϕ_{cr} are parameters related to permeability change.

For gas and water flow in the FC, van Genuchten-Mualem model is applied in the model [11,12]. The capillary pressure is written as

$$p_c=p_{fg}-p_{fw} \quad (15)$$

The effective water saturation is expressed by

$$S_e=\begin{cases}\left[1+\left(\frac{p_c}{p_{gev}}\right)^{\frac{1}{1-m}}\right]^{-m} & p_c>0 \\ 1 & p_c\le 0\end{cases} \quad (16)$$

where m is the model parameter, and p_{gev} is the gas entry value.

The relative permeability of water flow k_{rw}, gas flow k_{rg} is given as

$$k_{rw}=\sqrt{S_e}[1-(1-S_e{}^{1/m})^m]^2 \quad (17)$$

$$k_{rg}=(1-S_e)^3 \quad (18)$$

4. Model Validation

To evaluate the predictive ability of the developed double porosity model, the above derived equations are implemented into COMSOL Multiphysics® software, in which the mass balance equations, i.e., Eq. (5), (6), (7), are implemented through the Subsurface Flow Module, the constitutive equation, i.e., Eq. (12), is incorporated into the Solid Mechanics Module, Eq. (10) and (11) are implemented through ODE and DAE interface. The experimental data or results of gas injection test are used to validate the HM model.

4.1 COx-1 test

In order to better understand the gas migration process through the host rock, a gas injection test on Callovo-Oxfordian mudstone sample (COx-1) conducted by Harrington et al. [13] is adopted in the study. A schematic diagram of the apparatus is shown in Figure 2. The gas helium was injected into the COx-1 sample through an injection filter (IF). The water counterpressure was controlled as 4.5 MPa at the backpressure filter (BF). A constant confining pressure, i.e., 12.5 MPa, was applied onto the sample. When the injection process began, the pressures in the injection guard-ring (IGR) and the back-pressure guard-ring (BGR) can be monitored, which is useful to provide some additional information, i.e., pore pressure evolution, anisotropy of fluid flow [13].

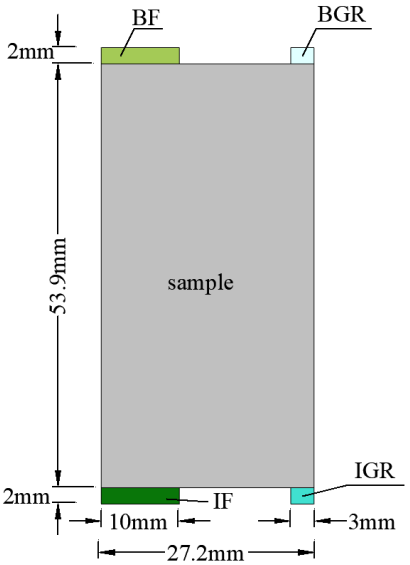

Figure 2. Schematic diagram of the test system

The injected gas pressure increased from 6.5 MPa up to the maximum value of 12 MPa in 7 steps and then decreased down to 7 MPa in two steps, as shown in Figure 3. The gas outflow rate is recorded under the standard temperature and pressure (STP) condition, see the data in Figure 3.

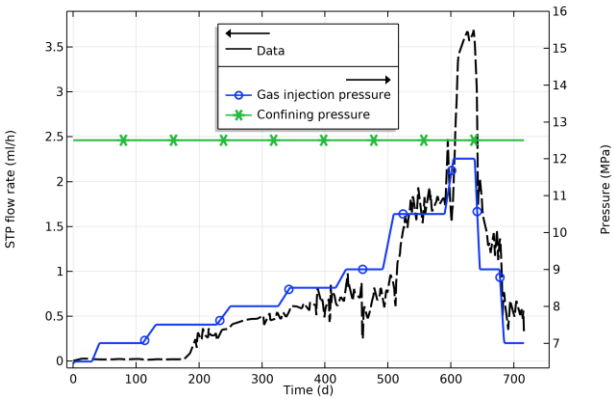

Figure 3. Applied pressure and recorded flow rate data in the experiment [13]

4.2 Parameters and boundary conditions

The parameters used in the simulation are extracted from [13,14] and listed as follows.

Table 1. Parameter values for modelling (note: subscript '0' denotes the corresponding initial value)

ρ_s , g/cm^3	2.31	G, MPa	769
ϕ_{f0}	0.04	K_p , MPa	1667
ϕ_{p0}	0.11	K_f , MPa	1500
S_{e0}	97%	b_1	72
$k_{f0//}$, m^2	3.5×10^{-19}	b_2	1
$k_{f0\perp}$, m^2	1.4×10^{-20}	ϕ_{cr}	0.0014
p_{gev} , MPa	1	ξ, m*s/kg	3×10^{-13}
m	1/3		

In the numerical model, the sample, IF and BF as well as the injection guard-ring (IGR) and the back-pressure guard-ring (BGR) were all included, see Figure 4. Due to the axisymmetric condition, only half of the sample was modeled, and Boundary No. 6 represents the symmetrical axial. The filters (i.e., the IF, BF) and guard-rings (i.e., the IGR and BGR) were modeled by using an equivalent porous material with high permeability and high porosity. To avoid convergence problems due to the inconsistent deformation between the sample and the filters, or guard-rings, mechanical conditions were only applied to the sample, see Figure 4(b).

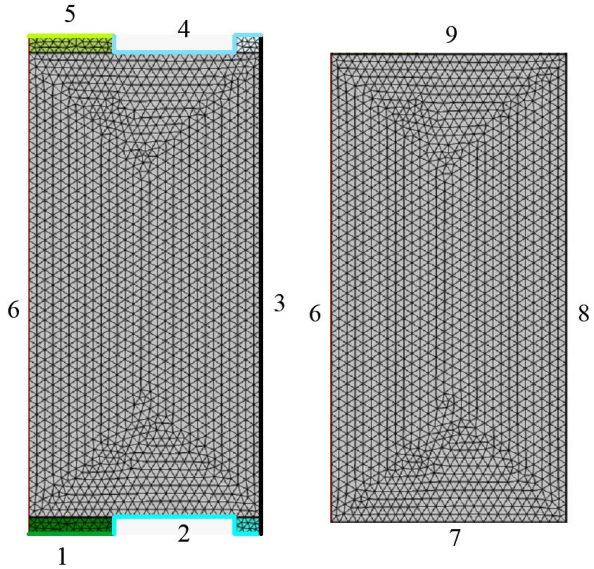

(a) Hydraulic BCs (b) Mechanical BCs

Figure 4. Geometry and BCs of the problem

The boundary conditions (BCs) for each module are tabulated in Table 2. The initial water pressure in the fractures and pores was set to 4.5 MPa, which is equal to the pressure in the BF. The initial gas pressure in the fractures was set to 4.71 MPa based on the initial water pressure and the degree of saturation. The initial effective stress was determined

to be -9.6 MPa. To obtain an equilibrium condition from the initial state, a ramp function was provided from 4.71 MPa to 6.5 MPa.

Table 2: BCs of HM model for COx-1 test

BC No.	Hydraulic boundary			Mechanical boundary
	Gas in FC	Water in FC	Water in PC	
1	Controlled pressure	No flow	No flow	-
2	No flow	No flow	No flow	-
3	No flow	No flow	No flow	-
4	No flow	No flow	No flow	-
5	4.71 [MPa]	4.5 [MPa]	No flow	-
6	Axisymmetric			
7	-	-	-	Roller
8	-	-	-	12.5 [MPa]
9	-	-	-	12.5 [MPa]

4.3 Experimental results and model validation

Figure 5 is a comparison between the numerically predicted and experimentally obtained gas outflow rate at STP condition. In general, the simulated results are in good agreement with the experimental data. However, it can be also found that the model slightly underestimates the flow rate when the gas pressure does not approach the maximum value, which reflects the difficulty to reproduce the dynamic gas pathway. The gas outflow rate increases in a stepwise manner that corresponds to the stepwise increase in the gas injection pressure. This shows that gas flows through the claystone along pressure-induced preferential pathways, which are likely to be governed by the increases in gas injection pressure at the inlet of the sample.

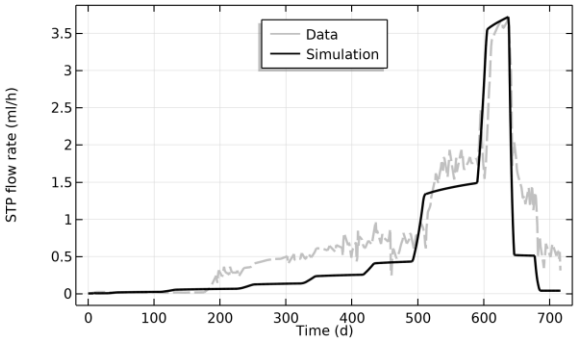

Figure 5. Gas outflow rate at STP

Figure 6 and Figure 7 show the comparisons between the numerically simulated and experimentally obtained results with respect to the IGR and the BGR pressure. The simulated gas pressure for the IGR is modeled well with the experimental data, while the simulated water pressure is closer to the BGR value. As the IGR is close to the injection inlet, water inside the IGR is replaced by gas quickly when the injection process begins. Thus the IGR pressure better fits the gas pressure. However, the BGR is close to the outlet, the BGR pressure is almost kept at 4.5 MPa when there is no development of new gas pathway propagating to the corner of BGR, see Figure 7.

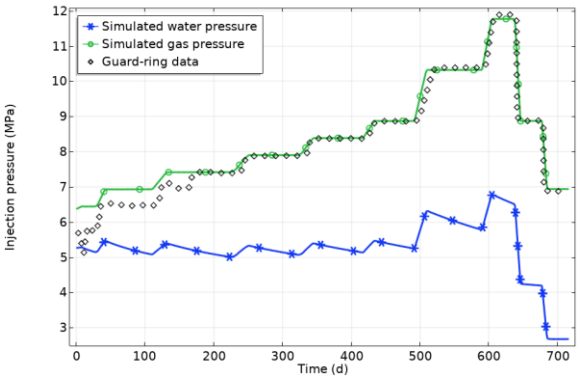

Figure 6. Pressure in the IGR

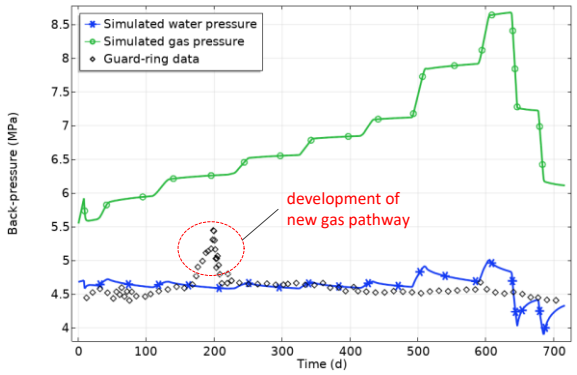

Figure 7. Pressure in the BGR

5. Conclusions

To capture the experimental observations of gas migration process, a coupled HM model with double porosity approach is developed. The model takes into account the HM behavior of both the porous medium (which represents the matrix) and the fractured medium (which is the fractures).. The developed model is evaluated against a gas injection test on COx-1. The simulated results are in good agreement with the experimental data.

However, the numerical model slightly underestimates the flow rate for low injection pressure, which confirms the difficulty of capturing the dynamic behavior of dilatant gas pathways. Further improvements can be made by introducing a 3D model with a non-symmetrical geometry and heterogeneous HM properties.

References

1. P. Marschall, T. Gimmi, S. Horseman, Characterisation of Gas Transport Properties of the Opalinus Clay, a potential host rock formation for radioactive waste disposal, *Science And Technology*, **60**, 121–139 (2005).
2. J.F.F. Harrington, R. de la Vaissière, D.J.J. Noy, R.J.J. Cuss, J. Talandier, Gas flow in Callovo-Oxfordian claystone (COx): Results from laboratory and field-scale measurements, *Mineralogical Magazine*, **76**, 3303–3318 (2012).
3. M. Fall, O. Nasir, T.S. Nguyen, A coupled hydro-mechanical model for simulation of gas migration in host sedimentary rocks for nuclear waste repositories, *Engineering Geology*, **176**, 24–44 (2014).
4. E.C. Aifantis, Introducing a multi-porous medium, *Dev. Mech*, **8**, 209–211 (1977).
5. S. Valliappan, N. Khalili-Naghadeh, Flow through fissured porous media with deformable matrix, *International Journal for Numerical Methods in Engineering*, **29**, 1079–1094 (1990).
6. D. Elsworth, M. Bai, Flow-Deformation response of dual-porosity media, *Journal of Geotechnical Engineering*, **118**, 107–124 (1992).
7. R. Nair, Y. Abousleiman, M. Zaman, A finite element porothermoelastic model for dual-porosity media, *International Journal for Numerical and Analytical Methods in Geomechanics*, **28**, 875–898 (2004).
8. Y. Abousleiman, V. Nguyen, Poromechanics response of inclined wellbore geometry in fractured porous media, *Journal of Engineering Mechanics*, **131**, 1170–1183 (2005).
9. R. Nair, Y. Abousleiman, M. Zaman, Modeling fully coupled oil-gas flow in a dual-porosity medium, *International Journal of Geomechanics*, **5**, 326–338 (2005).
10. J. Zhang, M. Bai, J.-C. Roegiers, Dual-porosity poroelastic analyses of wellbore stability, *International Journal of Rock Mechanics and Mining Sciences*, **40**, 473–483 (2003).
11. Y. Mualem, A new model for predicting the hydraulic conductivity of unsaturated porous media, *Water Resources Research*, **12**, 513–522 (1976).
12. M.T. van Genuchten, A closed-form equation for predicting the hydraulic conductivity of unsaturated soils, *Soil Science Society of America Journal*, **44**, 892–898 (1980).
13. J.F. Harrington, R.J. Cuss, J. Talandier, Gas transport properties through intact and fractured Callovo-Oxfordian mudstones, *Geological Society Special Publication*, **454**, 131–154 (2017).
14. M. Mahjoub, A. Rouabhi, M. Tijani, S. Granet, S. M'Jahad, J. Talandier, S. M'Jahad, J. Talandier, Numerical Study of Callovo-Oxfordian Argillite Expansion due to Gas Injection, *International Journal of Geomechanics*, **18**, 04017134 (2018).